Identification and Characterization of a Tetracycline Semiquinone Formed during the Oxidation of Minocycline

Mark J. Nilges,* W. Scott Enochs, and Harold M. Swartz

University of Illinois College of Medicine and Illinois EPR Research Center, Urbana, Illinois 61801

Received January 8, 1991 (Revised Manuscript Received June 15, 1991)

Oxidation of minocycline under slightly alkaline conditions produces a semiquinone free radical with hyperfine splittings that are atypical for a *p*-semiquinone. At high pH or on complexation with calcium and strontium, somewhat different spectra are observed, which are associated, respectively, with removal of the proton of the C-12 hydroxy group or with metal binding to the C-11–C-12 β-diketone system. The initial oxidation of minocycline is a two-electron process with no detectable free-radical intermediate. Hydrolysis of the dimethylamino group of this oxidation product yields a quinone. The reduced form of the quinone has been isolated and, by comparison of its NMR spectra to those of minocycline, has been identified as the quinol, 7-hydroxy-6-deoxy-6-demethyltetracycline. Complete analyses of the ^{1}H NMR spectra of both minocycline and 7-hydroxy-6-deoxy-6-demethyltetracycline are presented. Reverse dismutation of the quinone and its hydroquinone gives a *p*-semiquinone radical: the first reported tetracycline semiquinone. A hyperfine splitting of 7 G, which is atypical for a *p*-semiquinone, is attributed to an axial β-hydrogen proton adjacent to a position with a β-carbonyl group.

Introduction

Minocycline, 7-(dimethylamino)-6-deoxy-6-demethyltetracycline (1, $R^1 = N(CH_3)_2$, $R^2 = R^3 = R^4 = H$), is a semisynthetic derivative of tetracycline and is a more potent antibiotic than other tetracyclines.[1] Studies with laboratory animals have shown that high, daily doses produce thyroid pigmentation in rats, dogs, and monkeys but not in mice.[2] In addition, several cases of minocycline-induced pigmentation in surgical and autopsy specimens of human thyroid have been reported.[3] Skin pigmentation also has been reported in several patients on chronic minocycline therapy.[4] Although no direct toxic effects of minocycline-induced pigmentation have been reported, investigation of the nature and origin of such pigmentation is desirable, both to understand its pathophysiological significance and to minimize the potential for its occurrence.

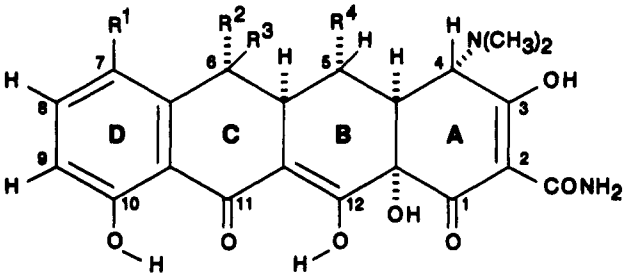

1

It is known that air oxidation of minocycline results in a dark pigment that gives a melanin-like EPR signal. One might postulate, therefore, that minocycline undergoes oxidation to a free-radical intermediate, which leads to polymerization of minocycline. As part of a systematic study to understand minocycline-induced pigmentation, we have looked for the formation of such a free radical during oxidation of minocycline and report here the characterization of the radical and the isolation of its parent compound. We also indicate the probable steps in the initial redox reactions of minocycline.

Experimental Section

Minocycline hydrochloride, Minocin, $C_{23}H_{27}N_3O_7 \cdot 2H_2O \cdot HCl$ (83.7% free base, 6.6% H_2O), was obtained as a gift from Lederle Labs. Horseradish peroxidase was obtained from Sigma. Benzoquinone was recrystallized from toluene. Because OH^- is consumed during the oxidation of minocycline, 0.1 M phosphate buffer solutions were used; for experiments with metal ions (in the form of chloride salts), KCl/NaOH buffer solutions were used.

EPR spectra were obtained at 9.76 GHz with a modulation amplitude of 0.125 G and a microwave power of 0.63 mW, unless otherwise noted. The *g* factors were determined by reference to the standard, tetraoxidobenzosemiquinone ($g = 2.004\,87$).[5] A stopped-flow system was used to observe transient radicals. Reactants were fed with syringes into a Plexiglas mixer and then directed into a quartz flat cell in a TM_{110} EPR cavity. A second mixer could be added to allow the initial reaction mixture to be mixed with a second reactant before being directed into the EPR cavity. The use of a stopped-flow system is convenient and facilitates quantitation of the time dependence of the EPR signal. Because the EPR signals of the radicals observed in this study decayed on a time scale as short as a minute, improved signal-to-noise was obtained by averaging the spectra from repeated mixings. All quantitative measurements were made with fresh solutions that were deaerated with nitrogen. EPR spectra were simulated by using the program RADI, which generates isotropic solution spectra.

UV–visible spectra were obtained with the stopped-flow system used for measuring EPR spectra after adaptation to direct the reaction mixture into a quartz cuvette instead of an EPR flat cell. Proton NMR spectra were obtained at 200 MHz with samples prepared as 1% solutions either in DMSO-d_6 (99.9 atom % D) or CD_3OD (99.96 atom % D), TMS being used as a reference.

Isolation of 7-Hydroxy-6-deoxy-6-demethyltetracycline (1, $R^1 = OH$, $R^2 = R^3 = R^4 = H$). Solutions of 276 mg of minocycline hydrochloride dihydrate in 100 mL of H_2O and of 444 mg of $K_3Fe(CN)_6$ in 100 mL of H_2O both were adjusted to pH 11.5; a solution of 176 mg of ascorbic acid in 100 mL of H_2O was adjusted to pH 9. The solutions of minocycline and ferricyanide first were mixed together in the stopped-flow apparatus described above, and this mixture was then directed into the second mixer for

* To whom correspondence should be addressed.

(1) Brogden, R. N.; Speight, T. M.; Avery, G. S. *Drugs* **1975**, *9*, 251.
(2) Benitz, K.-F.; Roberts, G. K. S.; Yusa, A. *Toxicol. Appl. Pharmacol.* **1967**, *11*, 150.
(3) (a) Attwood, H. D.; Dennett, X. *Br. Med. J.* **1976**, *2*, 1109. (b) Reid, J. D. *Am. Soc. Clin. Pathol.* **1983**, 738. (c) Bilano, R. A.; Ward, W. Q.; Little, W. P. *JAMA, J. Am. Med. Assoc.* **1983**, *249*, 1887. (d) Gordon, G.; Sparano, B. M.; Kramer, A. W.; Kelly, R. G.; Iatropoulos, M. J. *Am. J. Pathol.* **1984**, *117*, 98.
(4) (a) Basler, R. S. W.; Kohen, P. W. *Arch. Dermatol.* **1978**, *114*, 1695. (b) Simons, J. J.; Morales, A. M. *Am. Acad. Dermatol.* **1980**, *3*, 244. (c) Fenske, N. A.; Millns, J. L.; Greer, K. E. *JAMA, J. Am. Med. Assoc.* **1980**, *244*, 1103. (d) McGrae, J. D., Jr.; Zelickson, A. S. *Arch. Dermatol.* **1980**, *116*, 1262. (e) Sato, S.; Murphy, G. F.; Bernhard, J. D.; Mihm, M. C.; Fitzpatrick, T. B. *J. Invest. Dermatol.* **1981**, *77*, 264.
(5) Pederson, J. A. In *CRC Handbook of EPR Spectra from Quinones and Quinols*; CRC Press: Cleveland, 1985; pp 14–16.

0022-3263/91/1956-5623$02.50/0

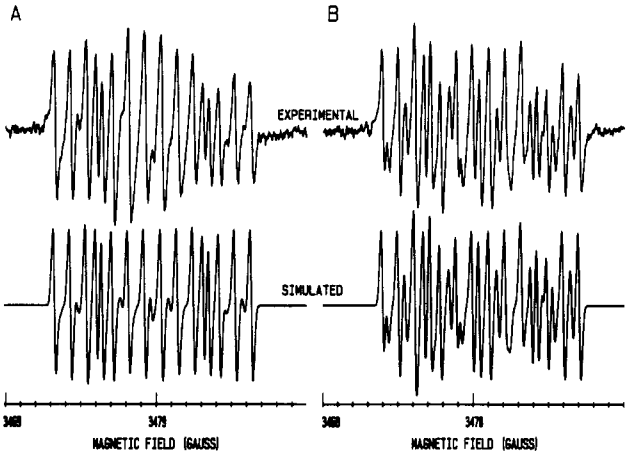

Figure 1. Experimental and simulated EPR spectra of the radical produced by oxidation of minocycline (2.0 mM) at pH 8.5 with $K_3Fe(CN)_6$ (2.0 mM). (A) Weakly buffered: $K_3Fe(CN)_6$ was dissolved in 0.25 mM buffer and minocycline in H_2O. (B) Strongly buffered: both $K_3Fe(CN)_6$ and minocycline were dissolved in 1.0 mM buffer. Modulation amplitude, 0.25 G; power, 6 mW; scan time, 8 min. Each spectrum is the average of six repeated mixings. The simulations make use of the parameters for radical **2a** reported in Table I for the primary species and hyperfine splittings of 6.19, 2.99, 1.96, and 1.24 G and g = 2.00477 for the secondary species, with a 10:1 ratio for A and a 2:1 ratio for B. The simulations assume a Gaussian line shape with ΔH_{pp} = 0.25 G.

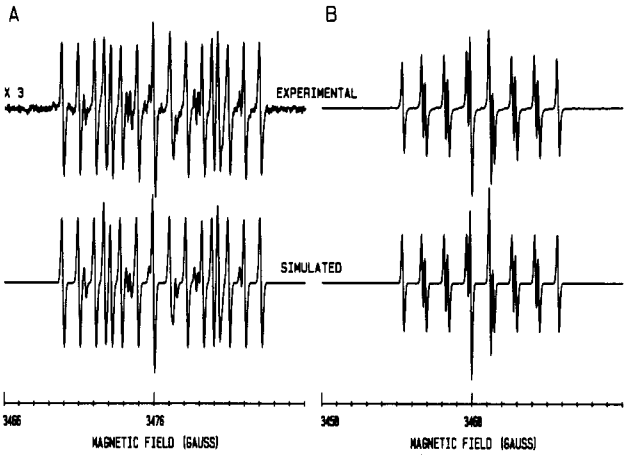

Figure 2. Experimental and simulated EPR spectra of the radical produced by oxidation of minocycline. (A) Minocycline (0.85 mM) and $K_3Fe(CN)_6$ (1.7 mM) were reacted at pH 11; scan time, 50 s. (B) Minocycline (1.0 mM) and $K_3Fe(CN)_6$ (1.0 mM) were reacted at pH 14; scan time, 20 s. Each spectrum is the average of five repeated mixings. The simulations make use of the parameters listed in Table I, with a mixture of **2a** and **2b** in a ratio of 6:1 for A and 100% of **2b** for B. The simulations assume a Gaussian line shape with ΔH_{pp} = 0.18 and 0.15 G for **2a** and **2b**, respectively.

reduction by ascorbate. Any unreacted minocycline was extracted with chloroform, and the solution was concentrated to 50 mL under vacuum and adjusted to pH 5 with HCl. This solution was placed in an ice bath, and the resultant precipitate was collected, washed, and dried. The crude product was redissolved in H_2O, filtered warm, and then cooled. This resulted in 30 mg of a yellow crystalline material. The best agreement between experimental and calculated microanalytical data was obtained by assuming 1.25 molecules of H_2O and 0.25 molecule of HCl of crystallization: λ_{max} (0.1 N HCl) 342 (log ϵ, 4.14) and 270 nm (log ϵ, 4.21).

Anal. Calcd for $C_{21}H_{22}N_2O_8 \cdot 1.25H_2O \cdot 0.25HCl$: C, 53.55; H, 5.51; N, 5.95; Cl, 1.88; O, 33.12. Found: C, 53.73; H, 5.95; N, 5.89; Cl, 1.97; O, 33.40 (balance).

Positive-ion fast atom bombardment (FAB) gave a parent peak at m/e 431 = $(M + H)^+$, and negative-ion FAB gave a peak at m/e 429 = $(M - H)^-$. High-resolution FAB gave a value of 431.1467 amu for the positive ion, compared to a calculated value of 431.1454 amu.

Results and Discussion

Autoxidation of minocycline under neutral conditions produces after several days a dark pigment, which shows a stable, symmetric EPR signal (g = 2.0040 and ΔH_{pp} = 4 G). Oxidation of minocycline is accelerated by increasing the pH and/or the addition of weak oxidizing agents. At pH above 8.5 and in the presence of potassium ferricyanide, oxidation of minocycline occurs within less than an hour, and a weak multiline EPR signal can be seen during this time. Other oxidizing agents that cause radical formation include potassium persulfate, sodium metaperiodate, ceric ammonium nitrate, lead dioxide, and silver oxide. Without an oxidizing agent present, even under strongly alkaline conditions, oxidation of minocycline is slow enough that no free-radical formation is detectable. Minocycline, which has a phenolic group at the 10-position, might be expected to form a phenoxy radical, especially with horseradish peroxidase,[6] yet no ready reaction or free-radical formation is seen when minocycline is flowed against a solution of horseradish peroxidase in the presence of H_2O_2 at a pH between 5 and 9.

The same EPR spectrum (Figure 1A) is observed for all oxidants and is due to four inequivalent protons having hyperfine splittings of 7.16, 2.82, 2.15, and 1.08 G. A weak second species is seen (Figure 1A) only at the very lowest pH's used and is dependent on buffer concentration, and if the stock solution of minocycline is made in buffer instead of distilled H_2O, this second signal can be quite strong, as shown in Figure 1B. The hyperfine structure of the second species also is due to four inequivalent protons, which have splittings of 6.19, 2.99, 1.96, and 1.24 G, and is attributed to formation of a degradation product of minocycline, most likely the C-4 epimer since the 6-deoxytetracycline, while being very stable, otherwise undergo reversible epimerization in the presence of buffers below pH 9.[7]

Acid–Base Equilibrium. At pH 11 and above, oxidation of minocycline is fairly rapid and, though the time duration of the signal is also much shorter, a much stronger EPR signal is observed (Figure 2A). The EPR signal of the species due to epimerization seen at lower pH's no longer is observed, but as the pH is increased above 11, a different signal is seen, which completely dominates the spectrum at pH 14 (Figure 2B). The hyperfine structure of this high-pH signal also results from four inequivalent protons, though with quite different hyperfine splittings of 4.53, 3.01, 1.50, and 1.29 G. The ratio of the concentrations of radicals is independent of the time course of the reaction and choice of oxidizing agent. A plot of the log of the ratio of the concentrations of the two radicals versus pH, shown in Figure 3, indicates that they are an acid–base pair having an apparent pK_a of 11.85.

The EPR spectra of both the acid and base forms of the radical are independent of whether the reaction is performed in H_2O or D_2O, indicating that the protons responsible for the hyperfine structure are nonexchangeable. Although the proton having a pK_a of 11.85 does not contribute to the hyperfine structure of the protonated radical, removal of this proton causes a marked change in the distribution of the unpaired spin density. This proton is assigned to the C-12 hydroxyl proton, since it is the only

(6) Shig, T.; Imaizumi, K. *Arch. Biochem. Biophys.* **1975**, *167*, 469.

(7) McCormick, J. R. D.; Jensen, E. R.; Miller, P. A.; Doerschuk, A. P. *J. Am. Chem. Soc.* **1960**, *82*, 3381.

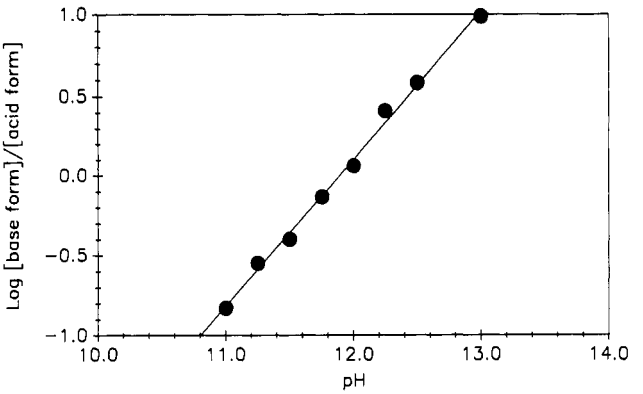

Figure 3. Plot of the logarithm of the ratio of the concentration of the base form of $P2^{\bullet-}$ (radical dianion **2b**) to that of its acid form (radical anion **2a**) as a function of pH. Concentrations were obtained by using the height of the low-field peak of each radical, after correction for the different ratios of height to double integral between the acid and base forms.

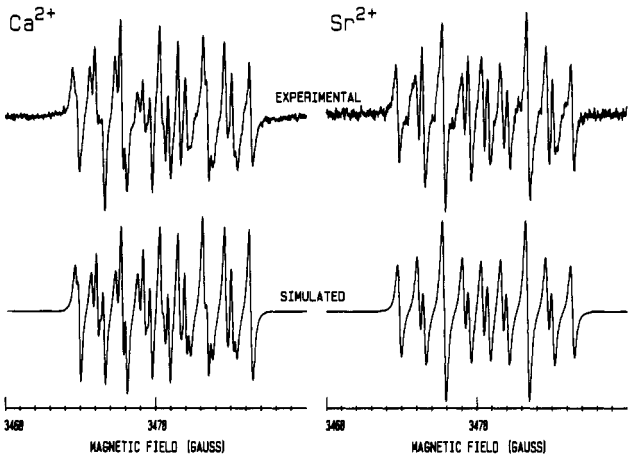

Figure 4. Experimental and simulated EPR spectra of the Ca^{2+} and Sr^{2+} complexed radicals at pH 12. The simulations make use of the parameters listed in Table I and assume a Lorentzian line shape with ΔH_{pp} = 0.24 G. (Minocycline, 0.85 mM; $K_3Fe(CN)_6$, 0.25 mM; and $CaCl_2$ or $SrCl_2$, 0.45 mM.)

exchangeable proton expected to affect the spin density on the aromatic ring, and yet have little spin density itself. (The quaternary proton on the C-4 dimethylamino group should have a pK_a between 9 and 10,[8] but removal of this proton is not expected to affect the spin density on the D ring because the A and D rings are not coplanar.[9,10]) Furthermore, the C-12 hydroxyl proton is strongly hydrogen bonded within the C-11–C-12 β-diketo group, especially after the removal of the C-10 hydroxyl, and is expected to have a high pK_a.[8b] This is exemplified by the pK_a of 11.5 for 10-(phenylsulfonyl)tetracycline,[11] in which the C-10 phenolic proton is replaced by a sulfonyl group.

Binding of Metal Ions. The formation of metal-complexed radicals can be observed (Figure 4) with both Ca^{2+} and Sr^{2+} when the pH is about 12 and the concentration of the metal binding is within the C-10–C-11–C-12 β-triketone group,[12] no definitive assignments can be made because of the number of different possible metal binding sites and stoichiometries expected for the tetracyclines.[12] Since the hyperfine splittings for the metal-complexed radicals lie between those for the acid and base forms of the uncomplexed radical, the hyperfine splittings for the latter two forms can be readily correlated (Table I).

Table I. EPR Parameters for the Semiquinone of 7-Hydroxy-6-deoxy-6-demethylteracycline Uncomplexed and Complexed with Metal Ions

	$a_{\beta'}$	$a_{\beta''}$	a_8	a_9	g	$a_{\beta''}/a_{\beta'}$
$P2^{\bullet-}$ (**2a**)	7.16	2.15	1.08	2.82	2.00471	0.30
$P2^{\bullet-}(Ca^{2+})^b$	5.89	1.62	1.09	3.08	2.00468	0.28
$P2^{\bullet-}(Ca^{2+})^c$	5.42	1.65	1.20	3.10	2.00465	0.30
$P2^{\bullet-}(Sr^{2+})$	5.56	1.67	1.30	3.00	2.00466	0.30
$P2^{\bullet-}$ (**2b**)	4.53	1.29	1.50	3.01	2.00467	0.28

[a] Hyperfine splittings in units of gauss. [b] Species b; 43%. [c] Species a; 57%.

Scheme I

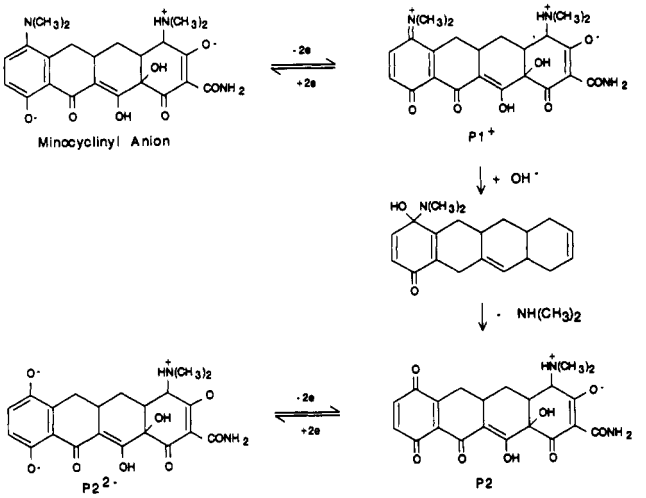

Formation Chemistry. For many tetracyclines, after prolonged incubation at high pH, a free radical is observed that is thought to result from aromatization of the A ring.[13] This is consistent with the tetracyclines having a C-6 hydroxyl group that can contribute to cleavage of the C ring in alkaline solution.[14] In contrast, minocycline does not have a C-6 hydroxyl group and a radical is observed almost immediately after reaction with only slightly alkaline ferricyanide, implying that this radical has the same basic skeletal structure as minocycline itself. Since radical formation for tetracycline (1, R^1 = H, R^2 = Me, R^3 = OH, R^4 = H) or chlortetracycline (1, R^1 = Cl, R^2 = Me, R^3 = OH, R^4 = H) is not observed under the same experimental conditions as those used for minocycline, the appearance of a radical from minocycline is linked to the presence of the C-7 dimethylamino group.

When ferricyanide is used as an oxidant, the value of the peak signal intensity scales linearly both with the concentration of reactants, up to a few millimolar, and with the molar ratio of the concentrations of ferricyanide to minocycline, up to a value of 2. At higher ratios of ferricyanide to minocycline, the peak signal intensity decreases and a lag time appears before the EPR signal is seen. This indicates that the initial oxidation of minocycline is a two-electron oxidation and that radical production occurs only after any excess ferricyanide has been

(8) (a) Leeson, L. J.; Krueger, J. E.; Nash, R. A. *Tetrahedron Lett.* **1963**, *1155*. (b) Rigler, N. E.; Bag, S. P., Leyden, D. E.; Sudmeier, J. L.; Reilley, C. N. *Anal. Chem.* **1965**, *37*, 872.

(9) Donohue, J.; Dunitz, J. D.; Trueblood, K. N.; Webster, M. S. *J. Am. Chem. Soc.* **1963**, *85*, 851.

(10) Cid-Dresdner, H. *Z. Kristallogr.* **1965**, *121*, 170.

(11) Stephens, C. R.; Murai, K.; Brunings, K. J.; Woodward, R. B. *J. Am. Chem. Soc.* **1956**, *78*, 4155.

(12) Brion, M.; Berthon, G.; Fourtillan, J. *Inorg. Chim. Acta* **1981**, *55*, 47.

(13) Lagercrantz, C.; Yhland, M. *Acta Chem. Scand.* **1963**, *17*, 2568.

(14) (a) Hochstein, F. A.; Stephens, C. R.; Conover, L. H.; Regna, P. P.; Pasternack, R.; Gordon, P. N.; Pilgrim, F. J.; Brunings, K. J.; Woodward, R. B. *J. Am. Chem. Soc.* **1953**, *75*, 5455. (b) Hlavka, J.; Schneller, A.; Krazinski, H.; Boothe, J. H., *J. Am. Chem. Soc.* **1962**, *84*, 1426.

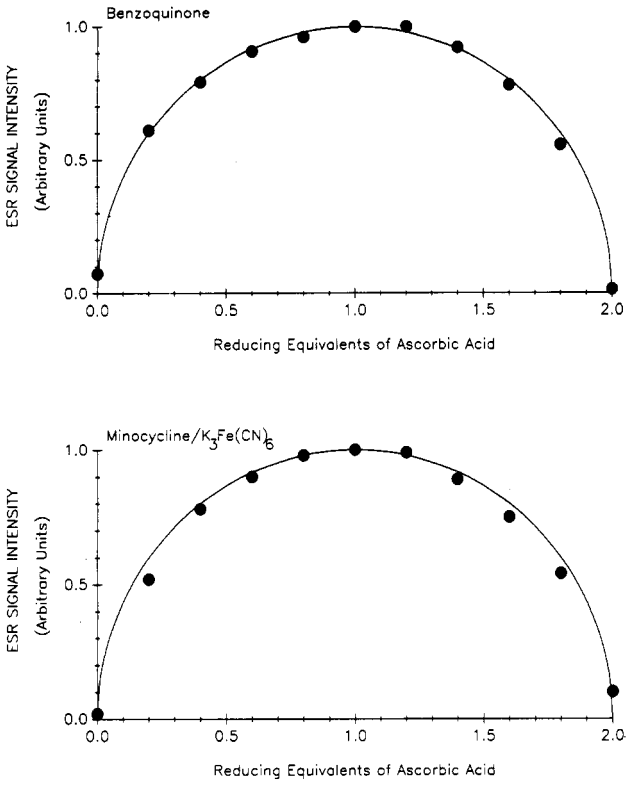

Figure 5. Plots of the EPR signal intensities of the benzosemiquinone radical and the radical produced from minocycline as functions of the number of equivlents of ascorbic acid used to reduce the parent quinones. Benzoquinone (1.0 mM) was reduced with ascorbate in pH 9 phosphate buffer. Minocycline (0.33 mM) was first reacted with $K_3Fe(CN)_6$ (0.33 mM) and then reduced with ascorbate at pH 11.

consumed in secondary reaction(s). These observations are best explained by Scheme I, in which the aromatic D ring of the minocyclinyl anion undergoes a two-electron oxidation to form a quinone imine cation $P1^+$, with subsequent addition of H_2O and elimination of dimethylamine to form the quinone P2, as inferred from polarographic studies.[15] The radical that is produced from the oxidation of minocycline is not believed to be the semiquinone imine $P1^\bullet$, the one-electron oxidation product of minocycline, since no nitrogen hyperfine splitting is observed. Not only would such a radical be destabilized by rotation of the dimethylamino group out of the aromatic plane, but the ready hydrolysis of $P1^+$ would cause the equilibrium value of $P1^\bullet$ to be negligible.

Redox Equilibrium. A more plausible assignment for the observed radical is the radical $P2^{\bullet-}$ (2), which can be formed by reverse dismutation of the quinone P2 and its two-electron reduction product $P2^{2-}$:

$$2P2^{\bullet-} \rightleftharpoons P2 + P2^{2-} \quad \text{and} \quad [P2^{\bullet-}]^2 = K[P2][P2^{2-}] \tag{1}$$

In general, the concentration s of a semiquinone as a function of the concentration x of the reductant used to titrate a quinone with initial concentration a can be approximated as[16]

$$s^2 \approx (k/4)(2 - x/a)(x/a), \text{ if } s \ll x \tag{2}$$

where the semiquinone formation constant k is equal to [S]/[R][T] and R and T represent all possible equilibrium

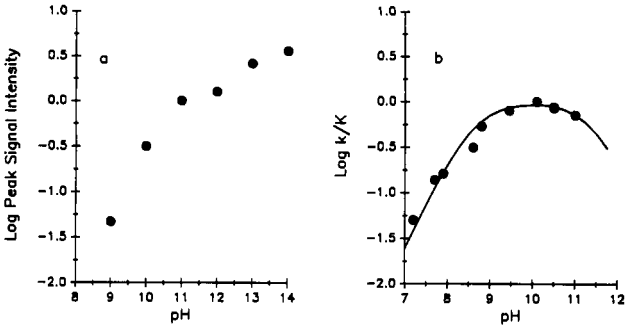

Figure 6. Peak EPR signal intensity as a function of pH: (a) Reaction of minocycline (0.85 mM) and $K_3Fe(CN)_6$ (0.85 mM) performed and measured at the indicated pH (the sum of the signal intensities of both the acid (**2a**) and base (**2b**) forms of the radical is plotted). (B) Reaction of minocycline (0.57 mM) and $K_3Fe(CN)_6$ (0.57 mM) first performed at pH 11 and then measured at the indicated pH. The curve for log k/K was calculated by using eq 3.

forms of the reduced and oxidized species, respectively (i.e., for P2, [R] = [$P2H_2$] + [$P2H^-$] + [$P2^{2-}$]). For benzoquinone[17] at pH 9, k is only 0.0016 so that $s \ll x$, and the titration data for benzoquinone in Figure 5 can be fitted readily with eq 2. Likewise, when minocycline is first oxidized by ferricyanide in the first mixer and then immediately reduced by ascorbic acid in the second mixer, the EPR signal is seen immediately and is a maximum when the concentration of ascorbate is one-half that of ferricyanide (Figure 5).[18] The titration data for minocycline can be similarly fitted to eq 2, confirming that the radical is produced by reverse dismutation of P2 and $P2^{2-}$.

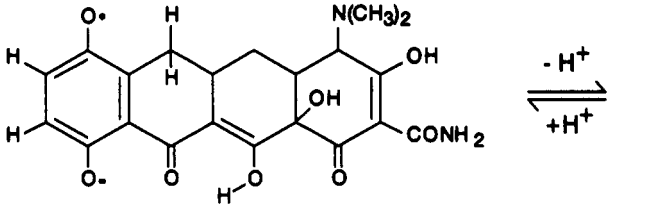

2a

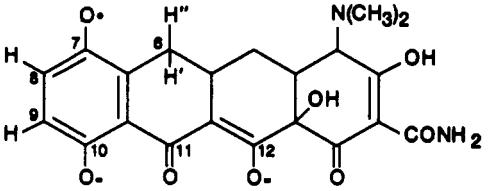

2b

pH Dependence of Radical Formation. The pH dependence of the EPR signal intensity of $P2^{\bullet-}$ (Figure 6a) should be a function not only of the pH dependence of the semiquinone formation constant for P2 but also of the rate of elimination of the C-7 dimethylamino group, which is expected to increase with $[OH^-]$.[19] When the oxidation first is performed at pH 11 and the pH of the mixture then is lowered immediately (by mixing with strong phosphate

(15) Chatten, L. G.; Fleischmann, M.; Pletcher, D. *J. Electroanal. Chem.* **1979**, *102*, 407.
(16) Michaelis, L. *J. Biol. Chem.* **1932**, *96*, 703.
(17) Bishop, C. A.; Tong, L. K. J. *J. Am. Chem. Soc.* **1965**, *87*, 501.
(18) The data shown in Figure 5 were obtained at minocycline concentrations of less than 0.50 mM. At higher concentrations, the data deviate from the simple curves shown in the figures. A 2-fold excess of minocycline was used for Figure 5 to avoid the lag time seen when the ratio of $K_3Fe(CN)_6$ to minocycline was greater than 2:1. The data were taken at pH 11 because the semiquinone formation constant for P2 is much smaller than that for most benzoquinones.
(19) Nickel, U.; Jaenicke, W. *J. Chem. Soc., Perkin Trans. 2* **1980**, 1601.

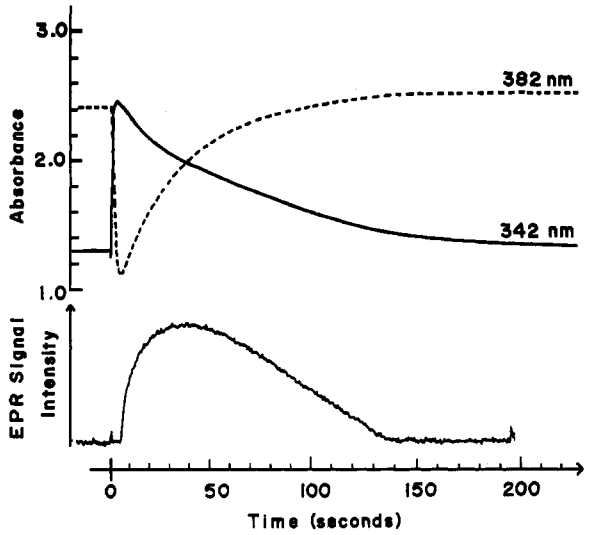

Figure 7. Comparison of the time dependencies of the absorbances at 382 and 342 nm with that of the EPR signal intensity during oxidation of minocycline (1.0 mM) and $K_3Fe(CN)_6$ (2.0 mM) at pH 11.

buffer in the second mixer), formation of $P2^{\bullet-}$ can be measured at a pH as low as 7 (Figure 6b), without observed formation of the additional species attributed to epimerization. The inability to observe $P2^{\bullet-}$ directly at pH less than 9 is due less to a low formation constant than to the slow rate of oxidation of minocycline to yield P2. The shape of the curve in Figure 6b is typical for benzoquinones:[17] the drop-off below pH 10 is due to protonation of the hydroquinone, while that above pH 10 is due to the reversible formation of a OH^- adduct with the quinone.

The semiquinone formation constant k is related to the semiquinone equilibrium constant K, defined in eq 1, as follows:[17]

$$k/K = (1 + [H^+]/K_2 + [H^+]^2/K_1K_2)^{-1}(1 + K_cK_w/[H^+])^{-1} \quad (3)$$

where K_1 and K_2 are the ionization constants for the hydroquinone, K_w is 10^{-14} for water, and K_c is the formation constant of the OH^- adduct. The data in Figure 6b can be fitted readily with this equation by using $pK_2 = 8.6$ and $K_c = 400$ ($pK_c + pK_w = 11.4$) and by neglecting the term in K_1, which implies a value for pK_1 of less than 7 (for tetracyclines,[8] the pK_a of the C-10 hydroxyl group is typically about 7.5, and that for minocycline[20] is 7.8). Because pK_1 and pK_2 for $P2^{2-}$ are smaller than those seen for benzohydroquinones,[17] the maximum semiquinone formation constant for P2 is seen at pH 10 instead of at the more typical values of 12–13.

Reactions of Secondary and Tertiary Products. The secondary product P2 is relatively unstable and could not be isolated. The UV–visible spectrum of the solution of minocycline obtained immediately after oxidation with ferricyanide at pH 11 shows four absorption maxima: 210, 244, 342, and 460 nm, with relative extinction coefficients of 1:29:36:50. The band at 342 nm disappears in time and is replaced by a new band at 382 nm with a shoulder at about 400 nm. When the absorptions at 342 and 382 nm are compared to the time dependence of the EPR signal, as shown in Figure 7, the initial oxidation of minocycline is seen to be complete within a few seconds and the buildup and decay of the radical are seen to be associated with disappearance of the band at 342 nm for P2 and appearance of a band at 382 assigned to $P2^{2-}$. This confirms that $P2^{\bullet-}$ is formed by reverse dismutation of P2 and $P2^{2-}$ and so has a maximum concentration when the reduction of P2 to $P2^{2-}$ is about 50% complete. Reduction of P2 to $P2^{2-}$ is autocatalytic: like other quinones, P2 will undergo nucleophilic addition readily to give extended hydroquinones that can then reduce additional P2, the efficacy for each depending on their relative concentrations and redox potentials. P2 could also be reduced directly by minocycline; however, the relatively high redox potential of minocycline[15] compared to $P2^{2-}$ limits the extent to which this can happen. On the other hand, several addition products with lower redox potentials can be postulated: A dimer can form by the coupling of two radicals at sites of high spin density and low steric hindrance (i.e., C-9) or by direct addition of $P2^{2-}$ to P2. At higher pH, conjugate addition of OH^- to P2 will occur: reversible addition of OH^- to the 7-position gives the adduct described in the preceding section, while irreversible addition to the 9-addition will result in a trihydroxy-substituted species. At lower pH, where the rate of oxidationn of minocycline is slow and P2 is produced at lower concentrations over a longer period of time, addition of P2 to the unreacted minocycline will result in mixed dimers and oligomers, which then can undergo further oxidation and addition, eventually leading to a polymer.

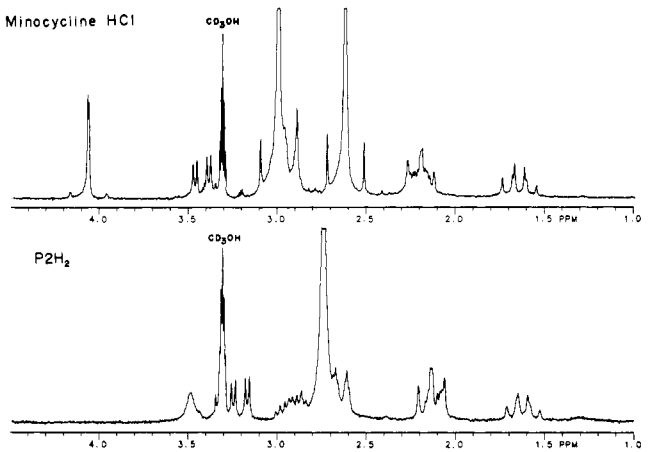

Figure 8. Proton NMR spectra of minocycline hydrochloride (**1a**·HCl) and $P2H_2$ (**1b**) obtained in CD_3OD (99.96% D). The singlets due to the dimethylamino protons at 2.62 and 2.99 ppm for minocycline and those at 2.87 ppm for $P2H_2$ have been truncated.

Proton NMR Spectra. The chemical analysis of $P2H_2$, which could be isolated by immediately reducing P2 with ascorbate, was consistent with identification of the compound as the hydroquinone **1b**, though more conclusive identification was obtained from proton NMR. The spectrum of minocycline has been reported[21] but has not been completely interpreted. We have found that the proton NMR spectra of minocycline hydrochloride (**1a**·HCl) and $P2H_2$ (**1b**) in deuterated methanol are very similar (Figure 8) except that, while the spectrum of **1a** has two strong singlets (2.62 and 2.99 ppm), each corresponding to six protons and assignable to the C-4 and C-7 dimethylamino groups, that of **1b** has only one such singlet (2.74 ppm). Another difference is that a mutliplet seen at 2.92 ppm in the spectrum of **1b** is obscured completely in that of **1a**.

(20) We have measured four macroscopic pK_a's for minocycline: pK_a's at 3.2, 7.8, and 9.3 are typical of tetracyclines[8] and have been attributed to the tricarbonyl system on the A ring, the phenolic β-diketone system, and the quaternary proton of the 4-dimethylamino group, respectively. An addition pK_a at 5.1 is attributed to the quaternary proton of the 7-dimethylamino group.

(21) Casy, A. F.; Yasin, A. *J. Pharm. Biomed. Anal.* **1983**, *1*, 281.

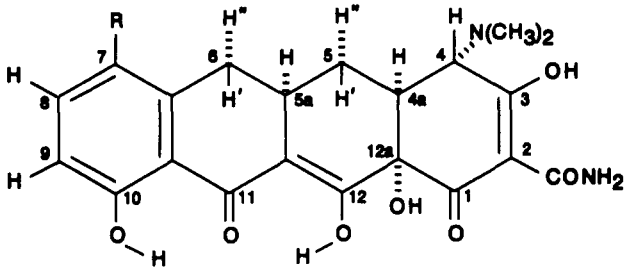

1a, R = $N(CH_3)_2$

1b, R = OH

The remaining structure in both **1a** and **1b** is attributable to protons at positions 4, 4a, 5a, 5′, 5″, 6′, and 6″, and this assignment is based on the reslts of several techniques. First, the area under the multiplet at 2.1 ppm for both compounds corresponds to two protons; addition of a few microliters of DCl to either sample splits this structure into a near triplet and a doublet of doublets of doublets. Second, using homonuclear spin decoupling, strong irradiation at 3.0 ppm in the case of **1a** results in a marked simplification of the spectrum: the small splitting at 4.06 ppm disappears and the multiplets at 1.64, 2.19, 2.20, and 3.42 collapse into doublets with splittings of about 14 Hz. This simplification is expected if the partially obscured doublet at 2.93 ppm and a multiplet that is completely obscured by the dimethylamino peak (but still is seen at 2.92 ppm in the spectrum of **1b**) correspond to the bridgehead protons, H-4a and H-5a, respectively. Decoupling of these protons would leave only the coupling between two sets of geminal protons, H-5′ to H-5″ and H-6′ to H-6″, which should be on the order of 15 Hz. Upon irradiation of the multiplet at 2.92 ppm in the spectrum of **1b**, the near quartet at 1.62 ppm collapses into a triplet, the doublet of doublets of doublets at 2.11 ppm into an unresolved multiplet, the near triplet at 2.13 ppm into a doublet, and the doublet of doublets at 3.21 ppm into a doublet. Thus, the multiplet at 2.92 ppm in the spectrum of **1b** must correspond to H-5a, since this is the only proton that can couple strongly to four protons, namely, H-5′, H-5″, H-6′, and H-6″.

The complete assignment (Table II) of peaks for H-4, H-4a, H-5, H-5a, and H-6 is made by invoking the dependence of vicinal proton couplings on the dihedral angle ϕ between the C–H bonds: $^3J = A + B\cos\phi + C\cos 2\phi$, where for cyclohexanes[22] $A = 7$ Hz, $B = -1$ Hz, and $C = 5$. For protons trans diaxial to each other, couplings on the order of 13 Hz are expected, while those between an axial proton and an equatorial proton should be on the order of 4 Hz. Thus, the protons at positions 5′, 5a, 6′, and 4a are to a first approximation mutually trans diaxial, while those at positions H-5″ and H-6″ are pseudoequatorial and have smaller couplings that should be more sensitive to deviations from $\phi = 60°$. The dihedral angles calculated from $J_{4a,5''}$, $J_{5a,6''}$, and $J_{5a,5''}$ of minocycline (70°, 59°, and 53°, respectively) correlate well with those calculated from the crystal structure of oxytetracycline (1, R^1 = H, R^2 = Me, R^3 = OH, R^4 = OH)[10] (67°, 54°, and 39°, respectively), despite the additional methyl and hydroxyl groups of the latter.

Exchangeable protons, which are not observed when CD_3OD is used, can be seen downfield from 8 ppm when tetracyclines are dissolved in DMSO.[23] Because the NMR data for **1b** in CD_3OD indicate that the isolated compound is the free-base form, the NMR spectrum of **1b** precipitated from dilute HCl also was recorded in order to make a proper comparison. The structures downfield from 8 ppm for both **1a** and **1b** in DMSO-d_6 again are very similar (Figure 9; Table III), except that an additional peak at 9.2 ppm, which is characteristic of an aromatic hydroxyl group, is observed in the latter between the two NH_2 peaks.

Thus, proton NMR indicates that **1b** has the same structure as **1a**, except for replacement of the C-7 dimethylamino group with a hydroxyl group. Furthermore, since the chemical shifts for the protons at positions 4, 4a, 5′, 5″, and 5a in the spectrum of the hydrochloride salt of **1a** are within a few percent of those typically reported for the hydrochloride salts of tetracycline and chlorotetracycline,[24] **1b** and **1a** also have the same basic conformation as the other tetracyclines,[9,10] though minor differences are present due to the lack of C-6 methyl and hydroxyl groups.

Hyperfine Coupling in EPR Spectra. Because $P2^{\bullet-}$ is the semiquinone of $P2H_2$ (**1b**) and can be generated directly from $P2H_2$ by oxidation with alkaline ferricyanide, the NMR data presented in the preceding section confirms that the radical produced from minocycline is $P2^{\bullet-}$ (**2**).

Table II. NMR Parameters for Minocycline Hydrochloride (1a·HCl) and $P2H_2$ (1b) in Methanol

	1a·HCl	1b
	Chemical Shifts (ppm)	
H-4	4.06 d (3.80)[a]	3.48 br s
H-4a	2.93 dt (2.27)[a]	2.64 dt
H-5′	1.64 dt	1.62 dt
H-5″	2.20 ddd	2.11 ddd
H-5a	2.9–3.0	2.92 m
H-6′	2.19 dd	2.13 dd
H-6″	3.42 dd	3.21 dd
H-8	6.81 d	6.61 d
H-9	7.44 d	6.99 d
4-$N(CH_3)_2$	2.99 s	2.74 s
7-$N(CH_3)_2$	2.62 s	
	Coupling Constants (Hz)	
$J_{4a,4}$	1.59	2.6
$J_{4a,5'}$	13.65	12.70
$J_{4a,5''}$	2.86	2.6
$J_{5a,5'}$	11.11	10.48
$J_{5a,5''}$	5.08	5.40
$J_{5a,6'}$	13.34	13.66
$J_{5a,6''}$	4.12	4.44
$J_{5',5''}$	13.65	13.65
$J_{6',6''}$	15.55	15.55
$J_{8,9}$	8.89	8.89

[a] Chemical shifts for minocycline as its free base.

Table III. NMR Parameters of Minocycline and $P2H_2$ in DMSO

	minocycline hydrochloride	minocycline free base	$P2H_2$	$P2H_2$/HCl
	Chemical Shifts (ppm)			
12-OH	14.8	14.6	14.7	14.89
10-OH	11.28	11.31	11.10	11.06
7-OH			9.23	9.2
NH_2'	9.52	9.10	9.10	9.33
NH_2''	9.07	8.7	8.5	9.05
H-9	7.42	7.39	7.04	7.02
H-8	6.84	6.80	6.66	6.68
	Coupling Constants (Hz)			
$J_{8,9}$	8.79	8.79	8.79	8.85

(22) Bothner-By, A. A. *Adv. Magn. Reson.* **1965**, *1*, 195.

(23) Asleson, G. L.; Stoel, L. J.; Newman, E. C.; Frank, C. W. *J. Pharm. Sci.* **1974**, *63*, 1144.

(24) Casy, A. F.; Yasin, A. *Magn. Reson. Chem.* **1985**, *23*, 767.

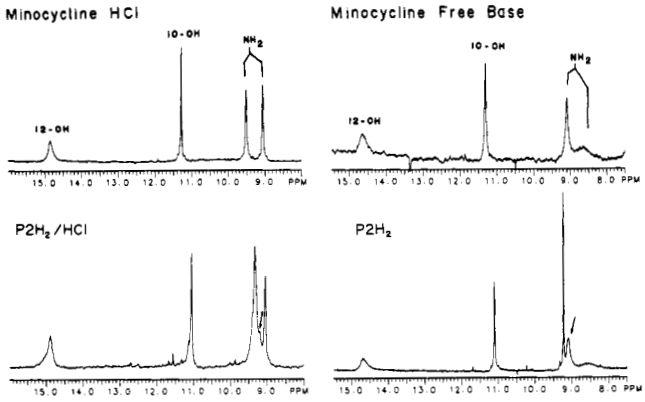

Figure 9. Proton NMR spectra of minocycline hydrochloride (**1a**·HCl) and its free base and those of $P2H_2$ (**1b**) and $P2H_2$ after precipitation from dilute HCl. Spectra were obtained in DMSO-d_6 and show exchangeable protons. Arrows mark additional peaks associated with a hydroxyl group at position 7.

Table IV. Hyperfine Couplings for 2-Carbonyl-Substituted Benzosemiquinones[a] versus 7-Hydroxy-6-deoxy-6-demethyltetracycline Semiquinones

	a_3	a_5	a_6	$(a_5 + a_6)/2$
benzosemiquinone[b]	2.35	2.35	2.35	2.35
carboxylato[b]	2.20	2.01	2.60	2.29
2-carbethoxy[c]	3.57	1.40	2.45	1.92
2-acetyl[c]	3.89	1.25	2.49	1.87
	$B/2$	a_8	a_9	$(a_8 + a_9)/2$
$P2^{\bullet-}$ (**2b**)	2.27	1.50	3.01	2.26
$P2^{\bullet-}$ (**2a**)	3.58	1.08	2.82	1.95

[a] Hyperfine splittings in units of gauss. [b] In water; ref 5. [c] In water/ethanol; ref 5.

The four hyperfine splittings can then be assigned to the two ring protons at positions 8 and 9 and the two β-hydrogens at position 6. However, the radical anion form (**2a**) of $P2^{\bullet-}$ shows a hyperfine splitting of 7 G, which is unusually large for a *p*-semiquinone; the latter has the majority of the spin density delocalized on the two C–O bonds[25] and has ring splittings that are typically only 1–3 G.[5] This large splitting can be explained, in part, by the fact that one β-hydrogen is nearly axial (cf. refs 9 and 10). The hyperfine coupling of β-hydrogen protons depends on the dihedral angle between the C–H bond and the π-orbital at the α-carbon according to the relationship[26] $a_\beta^H = B\cos^2\theta$. Thus, while a freely rotating methyl group ($\langle\cos^2\theta\rangle = {}^1/_2$) has a coupling of $B/2$, a rigid axial proton ($\theta = 0°$) will have a coupling equal to B and the complimentary proton ($\theta = 120°$) will have a coupling of $0.25B$, which will be sensitive to the dihedral angle. For all radicals reported in Table I, one splitting is always found to be 0.28–0.30-fold less than the largest observed splitting. These pairs of splittings, $a_{\beta'}$ and $a_{\beta''}$, can be assigned to the two protons at position 6, and dihedral angles of $\approx 2°$ and $\approx 122°$ can be calculated for them. From the crystal structure of oxytetracycline,[10] dihedral angles of $\approx -18°$ and $\approx 102°$ have been calculated for the hydroxyl and methyl groups, respectively, at position 6. For these angles, the smaller of the two β-hydrogen splittings is predicted to be much less than 1 G; however, this assumes that the conformation at the C-6 carbon does not change when the protons are replaced by methyl and hydroxyl groups, and there is no consistent way to assign the four proton splittings for all forms of $P2^{\bullet-}$, if the splitting is less than 1 G.

For the radical dianion **2b**, the calculated value of 4.5 G for B is typical for *p*-semiquinones. (For example, for 2-methyl *p*-semiquinone, a_β^H is equal to 2.1 G,[5] which corresponds to 4.2 G for B.) The large value of 7.1 G for B obtained for the radical anion **2a** can be explained by considering the coupling of the C-11 carbonyl to the aromatic ring. This coupling will be large since it is expected to vary as $\cos^2$ of the dihedral angle between the two π-systems and the C-11 carbonyl is nearly coplanar with the aromatic ring (cf. refs 8 and 9). In the case of the radical anion **2a**, the negative charge can be delocalized onto the C-11 carbonyl only if the unpaired electron is localized on the ring at the 6a-position. Since this favors structure **3a** over structures **3b** and **3c**, the spin density will be shifted from C-8 and C-10 to C-6a, and the largest splitting will be $a_{\beta'}$. On the other hand, delocalization of the π-system

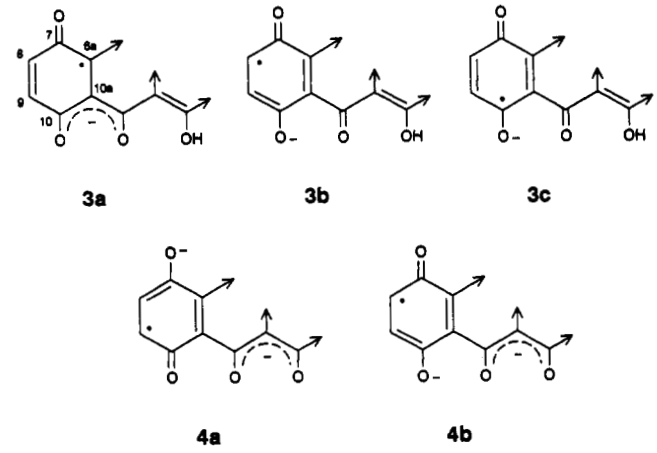

onto the planar C-11–C-12 β-diketo group will tend to decouple the C-11 carbonyl from the aromatic ring, particularly when the C-12 hydroxyl group is deprotonated. In the case of the radical dianion **2b**, negative charge can be delocalized readily onto the C-11–C-12 β-diketo group irrespective of the position at which the unpaired spin is placed, and the unpaired spin thus will be delocalized more uniformly on the ring. In this case, repulsion of the two negative charges will be greater with charge localized on the C-10 oxygen than on the C-7 oxygen. Since this favors structure **4a** over structure **4b**, the spin density will be shifted from C-8 to C-9 (with similar arguments for C-6a vs C-11a and C-10 vs C-7), and the largest splitting will be a_9. Delocalization of negative charge over the β-triketone system, whether it occurs on the C-10–C-11 portion or the C-11–C-12 portion, will always cause a decrease in a_8 and, additionally, will stabilize $P2^{2-}$ with respect to P2, which lowers the pK_a of the C-10 hydroxyl proton and raises the redox potential of $P2^{2-}$.

For 2-carbonyl-substituted *p*-semiquinones (Table IV), even though the substituent is rotating and $\langle\cos^2\theta\rangle \approx {}^1/_2$, a similar coupling of the carbonyl to the aromatic ring occurs, which is greatest for 2-acetyl substitution and is smallest for 2-carboxylato substitution. Since it has been found[27] repeatedly that $a_\alpha^H \approx -a_\beta^H = B/2$ for methyl substitution on π-radicals, $B/2$ and a_α^H both will be approximate measures of the spin density[28] at the adjacent carbon. Thus, the variation in $B/2$ for tetracycline semiquinones is comparable to that seen in a_3 for 2-substituted semiquinones (Table IV), and an increase in $B/2$ or a_3 correlates well with a decrease in $(a_8 + a_9)/2$ or $(a_5$

(25) Gulick, W. M., Jr.; Geske, D. H. *J. Am. Chem. Soc.* **1966**, *88*, 4119.
(26) Felix, C. C.; Sealy, R. C. *J. Am. Chem. Soc.* **1981**, *103*, 2831.
(27) (a) Kosman, D.; Stock, L. M. *J. Am. Chem. Soc.* **1969**, *91*, 2011. (b) Rabold, G. P.; Ogata, R. T.; Okamura, M.; Piette, J. H.; Moore, R. E.; Scheuer, P. J. *J. Chem. Phys.* **1967**, *46*, 1161.
(28) $\rho_n = a_n^H/Q_{CH}$, where $Q_{CH} \approx -27 \pm 3$ G.

+ a_6)/2, respectively. Moreover, as expected, the hyperfine splitting for either system is always smallest at the position opposite the substituent containing the carbonyl group.

Acknowledgment. This research was supported by NIH Division of Research Resources Grant RR-01811, NIH Department of Health and Human Services Traineeship (5 T32 CA 09067) to M.J.N., and Lederle Laboratories.

Registry No. **1a**·HCl, 13614-98-7; **1a**, 10118-90-8; **1b**, 61650-68-8; **1b**·$^1/_4$HCl, 135513-29-0; **2a**, 135513-28-9; **2b**, 135535-66-9; $K_3Fe(CN)_6$, 127435-14-7.

Synthesis of Self-Filled, Vaulted, and Intracavity-Functionalized Cappedophanes

Thottumkara K. Vinod and Harold Hart*

Department of Chemistry, Michigan State University, East Lansing, Michigan 48824

Received May 6, 1991

Two approaches to the synthesis of vaulted cappedophanes **3v** are described. In the first, the walls and ceiling were prefabricated as in tetrathiol **5** (**10a** and **10b**, Scheme II, are specific examples), which was then coupled with a *m*-terphenyl tetrabromide such as **4**. This route was most successful when the *m*-terphenyl base carried a large substituent (Ph, Br) in the 5′ position. Thus tetrathiol **10a** and tetrabromide **25** gave vaulted cappedophane **27v** in good yield (Scheme VIII). In the absence of a 5′ substituent, the major product was the self-filled conformer. For example, **10a** and **4** gave mainly **11sf** (62%) and only 2% of its vaulted conformer **11v** (Scheme III), and tetrathiol **10b** reacted with **4** to give (79%) only the self-filled conformer **15sf** (Scheme IV). In the second approach, a cuppedophane with suitably functionalized walls was first constructed, and the cap was attached in a second step. For example, bisphenol **29**, when coupled with *p*-xylylene dibromide, gave mainly vaulted conformer **11v** (51%) and only a trace of **11sf** (Scheme IX). Extension of this method to several other dihalides, however, gave mainly self-filled conformers (Schemes XI and XII) and even *p*-xylylene dibromide gave only self-filled product **33sf** when the bisphenol contained a substituent at $C_{2'}$ of the *m*-terphenyl base (Scheme XIII). The reasons for the predominant formation of self-filled vis-a-vis vaulted cappedophane conformers are discussed. These studies open the way for the synthesis of vaulted cappedophanes containing functionality within the molecular cavity.

We recently described efficient routes to two new classes of *m*-terphenyl-based cyclophanes **1** and **2**, called respectively *cuppedophanes* and *cappedophanes*.[1] The one-pot tandem aryne route[2] to the *m*-terphenyl moiety of **1** and **2** permits the direct introduction of substituents E at $C_{2'}$

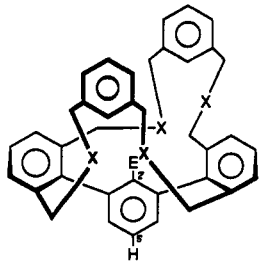

1 (X=S, SO_2, NTs, NH, —)

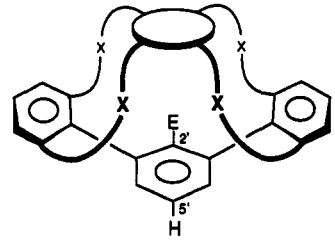

2 (X=S, SO_2, —)

and was used to prepare cuppedophanes with a substituent inside the "cup".[1b,3] In our first cappedophanes, however, the links between the *m*-terphenyl base and the cap were too short (only 2 or 3 atoms) to permit an E larger than a proton to be incorporated.

One goal of the present work was to enlarge the cavity in cappedophanes sufficiently to permit a functional group to be included at $C_{2'}$. This would permit a comparison of functional group chemistry within and outside a specifically designed microenvironment. To do this, the lengths

Scheme I

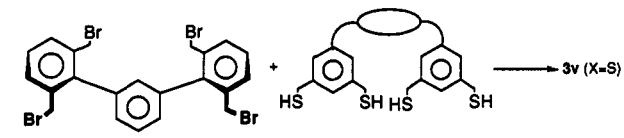

4 5

of the links would have to be increased. They would also have to be stiffened, because flexible links might allow collapsed conformations,[4] which would diminish the cavity volume.

The design we employed for this purpose is shown in **3v**, where a cap is added to the rigid walls of a cuppedophane to produce a vaulted cappedophane. We describe

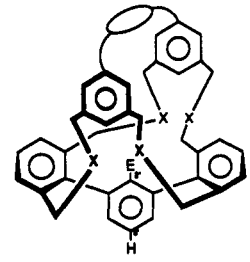

3v

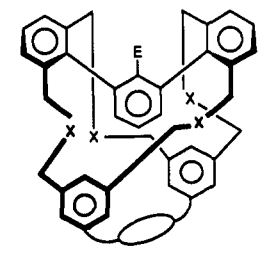

3sf

here several successful syntheses of this type. During this work, we also encountered a remarkably high propensity for the formation of **3sf**, a conformer of **3v** in which the central ring of the *m*-terphenyl moiety fills the molecular cavity. The relative energies of **3v** and **3sf** and factors that

(1) (a) Vinod, T. K.; Hart, H. *J. Am. Chem. Soc.* **1988**, *110*, 6574–6575. (b) Vinod, T.; Hart, H. *J. Org. Chem.* **1990**, *55*, 881–890. (c) Vinod, T. K.; Hart, H. *J. Org. Chem.* **1990**, *55*, 5461–5466.

(2) Du, C.-J. F.; Hart, H.; Ng, K.-K. D. *J. Org. Chem.* **1986**, *51*, 3162–3165. Du, C.-J. F.; Hart, H. *J. Org. Chem.* **1987**, *52*, 4311–4314.

(3) Our methodology was recently used by others for the same purpose, see: Lüning, U.; Wangnick, C.; Peters, K.; von Schnering, H. G. *Chem. Ber.* **1991**, *124*, 397–402.

(4) For examples, see: Jarvi, E. T.; Whitlock, H. W. *J. Am. Chem. Soc.* **1982**, *104*, 7196–7204.

0022-3263/91/1956-5630$02.50/0